

# Crossing microfluidic streamlines to lyse, label and wash cells†

Keith J. Morton,<sup>a</sup> Kevin Louterback,<sup>a</sup> David W. Inglis,<sup>‡a</sup> Ophelia K. Tsui,<sup>b</sup> James C. Sturm,<sup>\*a</sup> Stephen Y. Chou<sup>a</sup> and Robert H. Austin<sup>c</sup>

Received 15th April 2008, Accepted 2nd July 2008

First published as an Advance Article on the web 23rd July 2008

DOI: 10.1039/b805614e

We present a versatile method for continuous-flow, on-chip biological processing of cells, large bio-particles, and functional beads. Using an asymmetric post array in pressure-driven microfluidic flow, we can move particles of interest across multiple, independent chemical streams, enabling sequential chemical operations. With this method, we demonstrate on-chip cell treatments such as labeling and washing, and bacterial lysis and chromosomal extraction. The washing capabilities of this method are particularly valuable because they allow many analytical or treatment procedures to be cascaded on a single device while still effectively isolating their reagents from cross-contamination.

## Introduction

We present a methodology for moving selected particles across functional laminar streamlines in pressure-driven microfluidic flow using an asymmetric post array.<sup>1</sup> By directing objects into and through functional streamlines, complex biological objects can be lysed, labeled and analyzed on-chip without cross-contamination. In normal laminar flow, the migration of objects like cells across streamlines is limited by their slow diffusion in water.<sup>2–4</sup> Here, we use “deterministic lateral displacement” arrays to move cells across adjacent, parallel streams of reagents. We establish this concept by showing on-chip immunofluorescent labeling of platelets followed by washing, and, in a separate demonstration, show cell lysis with simultaneous chromosomal separation from the cell contents. These examples demonstrate the potential to implement sequential, chemical treatments on-chip by continuous flow manipulation of cells, large bio-particles, and functional beads.<sup>5–8</sup>

A number of techniques have been developed to enhance on-chip mixing of diffusive chemical species,<sup>9–11</sup> but these techniques irreversibly mix the contents, contaminate downstream treatments, and have limited use for species that diffuse slowly, such as cells, beads, and large biomolecules. In our approach, we send particles and fluids through an asymmetric array of posts; each successive row is shifted relative to the previous row so that the array axis forms an angle  $\alpha$  with respect to the channel walls that defines the average fluid flow direction. During operation, particles greater than some critical size set

by the device geometry are displaced laterally at each row by a post and follow a deterministic path through the array in the “bumping” mode. The trajectory of bumping particles follows the array axis which differs from the flow direction by an angle  $\alpha$ , shown schematically in Fig. 1(a). Particles smaller than the critical size follow the fluid streamlines and travel along the average fluid flow direction. This method is relevant for the high Peclet number, low Reynolds number flows that characterize many continuous-flow microfluidic devices<sup>12</sup> and adds to a number of other on-chip manipulation techniques available for studying biological systems.<sup>13–16</sup> Here, we perform on-chip particle treatments by moving targeted particles, such as bacteria and platelet cells from human blood, across multiple, parallel streams of reagents.

In a first example, we use the array to direct fluorescent beads across streams of smaller beads. Fig. 1(b) shows a time trace of 3.0 micron diameter fluorescent beads crossing a stream of 0.5 micron fluorescent beads in a device with a critical particle size of 2.4 microns. The larger beads travel along the angle  $\alpha$  in what we refer to as the bumping mode—in this example, the array angle is 11.3°—while the smaller beads follow the overall fluid flow and can be used as a streamline trace. Despite similar and small diffusion constants relative to water ( $D_{3.0\mu\text{m}} \sim 1.5 \times 10^{-9} \text{ cm}^2 \text{ s}^{-1}$ ,  $D_{0.5\mu\text{m}} \sim 9 \times 10^{-9} \text{ cm}^2 \text{ s}^{-1}$ ) the larger particle enters, is immersed in and then quickly exits the particle stream [ESI video M1†]. The residence time of a bumping particle in a reagent stream can be increased by increasing the width of the stream at the input or changing the array parameters so that the particle drops below the critical particle size; it will then stay in the stream until the array is changed back so that the particle is above the critical particle size. Alternatively, the residence time can be decreased by decreasing the width of the stream at the input or increasing the flow speed.

Directing a particle across a stream of other particles with a slightly larger diffusion coefficient demonstrates the unique capabilities of this method. However, the more common case for cell treatments will be moving a particle across species with much higher diffusion constants than that of the target

<sup>a</sup>Princeton Institute for the Science and Technology of Materials (PRISM), Department of Electrical Engineering, Princeton University, NJ, USA. E-mail: sturm@princeton.edu

<sup>b</sup>Department of Physics, Boston University, Cambridge, MA, USA

<sup>c</sup>Princeton Institute for the Science and Technology of Materials (PRISM), Department of Physics, Princeton University, NJ, USA

† Electronic supplementary information (ESI) available: Supplementary text, Fig. S1 and S2, and videos M1–M5. See DOI: 10.1039/b805614e

‡ Current address: Department of Physics, Macquarie University, NSW, Australia.

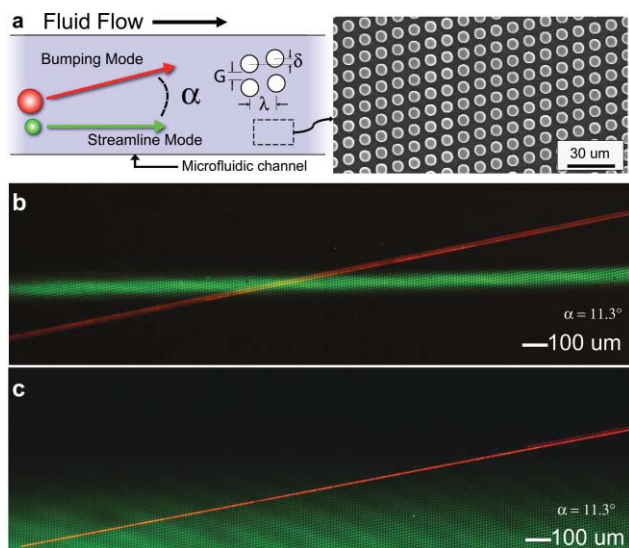


**Fig. 1** Directing beads across non-mixing laminar streams. (a) A microfabricated post array can be used to separate particles by size by making the array asymmetric with respect to the flow direction; here, the array is tilted at an angle  $\alpha$  relative to the channel walls and bulk fluid flow. This element directs particles larger than a critical size along a trajectory at an angle to the flow in the “bumping mode” while particles smaller follow the overall flow along streamline paths that weave through the posts. (Inset) SEM image showing the top view of the microfabricated element with an array angle of  $\alpha = 11.3^\circ$ . (b) Epifluorescent time exposure of  $3.0\ \mu\text{m}$  beads (red) crossing over a stream of  $0.5\ \mu\text{m}$  beads (green) [Accompanying ESI video M1†]. (c) Frame sum of a  $3.0\ \mu\text{m}$  fluorescent bead (red) escaping from an area of high Rhodamine 6G dye concentration (green) into a coflowing region with no dye. [ESI video M2†].

particle. In this case, it is important that cross contamination between reagents be reduced by washing a particle of all previous treatments before entering the next reagent stream. An example of on-chip washing is shown in Fig. 1(c) (and ESI video M2†). This figure shows a frame sum of a  $3.0\ \mu\text{m}$  fluorescent bead (red) escaping from a region of high Rhodamine 6G (Exciton, Dayton, OH) dye concentration (green) into an adjacent region of no dye. In the  $8.0\ \text{s}$  that it takes the bead to traverse the  $2.5\ \text{mm}$  wide panel, it is vertically displaced  $500\ \mu\text{m}$  by the post array. In the same time frame, the Rhodamine 6G stream ( $D_{\text{R6G}} \sim 2.8 \times 10^{-6}\ \text{cm}^2\ \text{s}^{-1}$ ) is expected to broaden by  $65\ \mu\text{m}$ . It is clear from the figure that the bead has been transported from a region of high dye concentration to a region of low dye concentration. (It is possible that a particle carries some solvent from one stream with it after it passes through a stream into the next, but this effect is expected to be minor and has not yet been investigated.) Taken together, the two examples in Fig. 1 demonstrate that we can efficiently transport particles between distinct, non-mixing functional zones.

## Results and discussion

Labeling and washing target cells are common protocols for many bio-analysis techniques. Here we demonstrate that blood platelet cells can be fluorescently labeled and then immediately washed directly on-chip. Platelet cells are easily obtained and readily stain with immunofluorescent dye. We use the array first

to mix unlabeled platelets with a labeling dye and then to rinse them in buffer. The array ( $\alpha = 5.7^\circ$ ,  $G = 5\ \mu\text{m}$ ,  $\lambda = 20\ \mu\text{m}$ ) is designed so that blood platelets travel in the bumping mode into a stream of phycoerythrin (PE) conjugated CD-41 antigen (PE-CD41, eBioscience) which binds to the cell surface, and out into a washing stream. Fig. 2(a) is a video frame still showing freshly labeled platelets exiting a horizontal labeling jet. The platelet cells maintain a single trajectory along the array angle, encountering three distinct regions: The running buffer, which is the platelet source; the immunofluorescent labeling jet; and the washing buffer. Unlabeled platelets enter the labeling jet, pick up surface label and then are washed of residual dye on exit. Platelet motion relative to the dye flow is highlighted using a false-color composite (Fig. 2(b)) of averaged dye flow (red) and moving platelets (green). This label and wash treatment is a rudimentary demonstration of the possibilities for on-chip cell treatment. Another or many more reaction streams could be cascaded with sufficient space between them for washing.

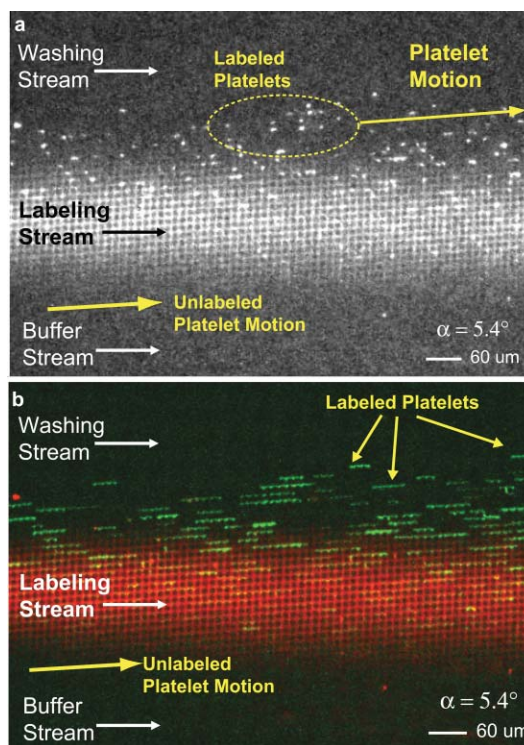


**Fig. 2** On-chip cell labeling with washing. (a) Blood platelets are directed across three coflowing reagent streams (running buffer, labeling dye and washing buffer) using the asymmetric array. Initially unlabeled platelets (not seen) move from the running buffer along a trajectory of angle  $\alpha = 5.7^\circ$  into a stream of fluorescent, surface-binding antigen (phycoerythrin-conjugated CD41). The freshly labeled platelets then continue through into the wash buffer and are delivered downstream [ESI video M3†]. (b) False-color overlay highlighting platelet motion relative to the dye. Red channel: Average of 20 video frames, showing CD41-PE labeling jet with running buffer below and washing buffer above. Green channel: Sum of 5 frames of platelet movement after subtracting the averaged dye flow used for the red channel. Merging the red and green channels captures the movement and tracking angle of the labeled platelets as they exit the dye and are washed.

A more sophisticated example of the cell processing and separation capabilities using these micropost arrays can be seen

in the continuous flow lysis (Fig. 3) and chromosomal separation (Fig. 4) of *E. coli* bacteria. In Fig. 3, two co-flowing streams of buffer each occupy one half of an array ( $\alpha = 5.7^\circ$ ,  $G = 1.4 \mu\text{m}$ ,  $\lambda = 8 \mu\text{m}$ ). The liquid in the lower section is TE buffer with 1.1 M sucrose while the upper section is the same with 8% SDS, a common lysing agent. Cells, following the tilt angle of the array, move from the lower region where they are osmotically stressed by the sucrose to the upper region where the SDS completes the lysis step (Fig. 3(a) and ESI video M4†). We used *E. coli*

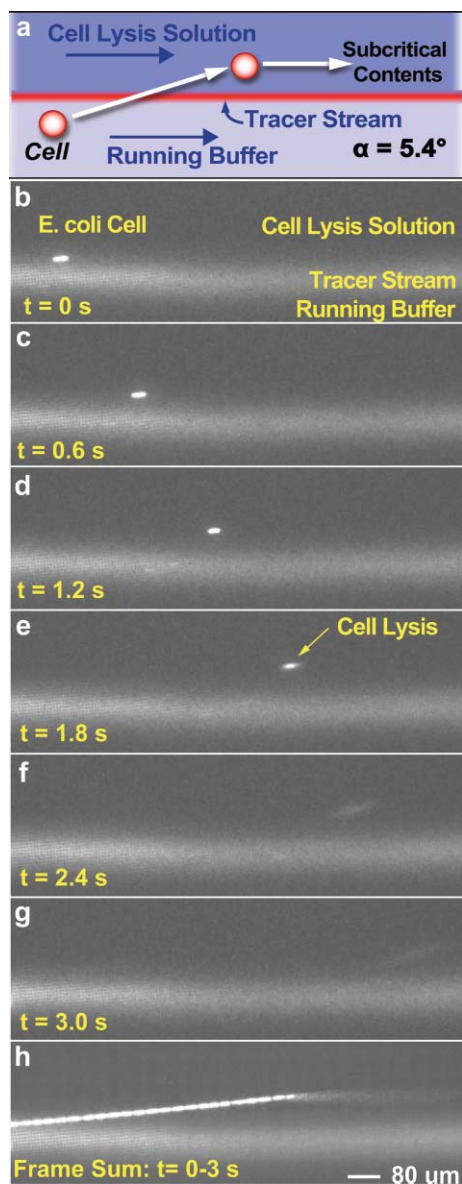


**Fig. 3** Continuous flow, on-chip cell lysis. A spheroplasted *E. coli* cell is directed across a tracer stream (GFP) and into a region of coflowing lysis solution along a trajectory of angle  $\alpha = 5.7^\circ$ . (a) Schematic of cell path from the lower half of the device containing a stream of sucrose and TE buffer into the upper half of cell lysing solution (8% SDS). A tracer stream delineates the two regions. After cell lysis, the GFP released from the cell travels parallel to the tracer stream and along the direction of fluid flow because it is below the critical size for bumping of 700 nm. Panels (b)–(g): Time sequence of cell lysis. Images are 0.6 s apart with a 100 ms shutter speed. Panel (h) shows an open-shutter montage of 3 s of the motion [Accompanying ESI video M4].

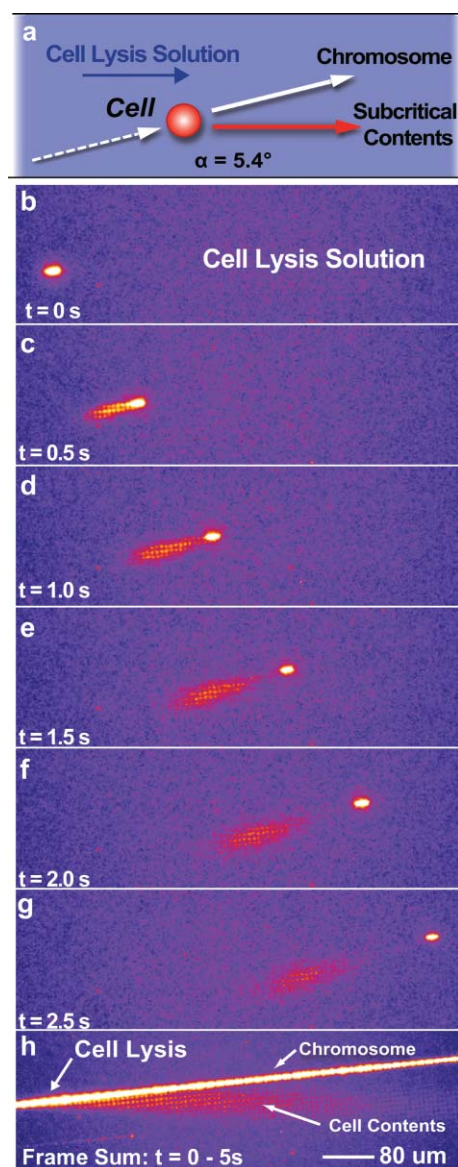


**Fig. 4** Lysis of a doubly-labeled, spheroplasted *E. coli* cell as it moves through a lysis solution of 8% SDS. (a) Schematic showing paths taken by various cell components before and after lysis. The chromosome of the GFP-expressing *E. coli* was fluorescently labeled (Syto13, Invitrogen) to allow tracking of chromosome trajectory in addition to other cellular components, which are visualized by the GFP. Panels (b)–(g): False-color time sequence of cell lysis. After lysis, the chromosome continues to track along the bumping trajectory, separating from the rest of the cell lysate which moves straight ahead. Here, color is applied (ImageJ, NIH) to highlight the path differences between the GFP in the cell debris and the brighter chromosome and to draw a distinction with Fig. 3 which showed a GFP tracer stream that is not shown here. Images are 0.5 s apart with a 100 ms shutter speed. Panel (h) shows an open-shutter montage of 5 s of the motion [ESI video M5].

with a green fluorescent protein (GFP) expressing plasmid to track cells and visualize lysis in real time. Furthermore, the *E. coli* were made into spheroplasts by removing the cell wall with lysozyme to increase lysis efficiency.<sup>18,19</sup> Fig. 3(b)–(g) shows the lysis of a single cell in the lysis buffer. The two regions, one with lysing agent and one without, are demarcated by the fluorescent tracer stream. As the cell moves through the array,

it is directed into the lysis buffer along the bumping trajectory. Once in the lysis buffer, the cellular membrane perforates and the cytoplasm empties out. Most of the cellular contents are smaller than the critical particle size, so they change trajectory after lysis.

This path can be visualized by the GFP since it is also below the critical particle size and will follow the same path as the rest of the subcritical cellular contents.

While this result demonstrates the capabilities for using a post array to lyse cells on chip, we are also interested in the trajectory of the *E. coli* chromosome once it is released from the cell. To visualize and track the chromosomes after lysis, the nucleic acid stain SYTO 13 (Invitrogen Corporation, Carlsbad, CA) was applied to an identical population of the cells used in the previous step. Fig. 4(b)–(g) shows the trajectory of the cellular components after lysis. As before, the small cellular contents, as visualized by the GFP, exit the bumping trajectory and follow the fluid flow after lysis. The chromosome, seemingly larger than the critical particle size, continues along the bumping trajectory of the original cell. The critical particle size in this chip was determined to be around 700 nm using fluorescent beads as a control standard. A frame sum (panel h) shows the separation clearly, with the angle between the GFP trace and the chromosome trace lines matching the tilt angle of the device. While both the GFP and SYTO13 dye appear green under 488 nm excitation, the absence of the fluorescent trail in Fig. 3 and other cells without the nucleic acid stain strongly suggests that the fluorescent particle tracking along the original cell path in Fig. 4h is, in fact, the intact chromosome separating from the cellular debris. In this simple setup, there were only two streams, but ongoing work seeks to add a third wash stream where the chromosomes can be collected for analysis or transported to another functional region downstream.

We now describe some fundamental and practical considerations for the design of a successful device. An array can be designed to move select particles across streamlines based on their size. The critical particle size depends primarily on the tilt angle, post spacing, and gap size<sup>20,21</sup> but not the fluid velocity. To avoid clogging, the gap  $G$  between the posts must be somewhat larger than the largest particle size. The threshold size to bump particles (as a fraction of the gap size) has been measured over a wide range of array angles:<sup>20</sup> For the array angles  $2.3^\circ$  and  $12^\circ$  (0.04 and 0.2 radians) the critical particle diameters are  $0.2 G$  and  $0.6 G$  respectively. Smaller angles have the advantage that the critical particle size is a smaller fraction of the gap. This reduces the chance of clogging, but the lateral particle displacement (with respect to the lateral diffusion of reagent) is not as rapid. Arrays have been constructed with critical sizes from 100 nm to 30  $\mu\text{m}$ .<sup>22,21</sup> Polystyrene beads, biomolecules, DNA,<sup>1</sup> yeast (unpublished) and human blood cells<sup>21</sup> (lymphocytes, erythrocytes and platelets) have all been successfully “bumped”.

In practice, we have found array angles between  $2.0^\circ$  and  $12^\circ$  to be the most useful. For particles in the bumping mode, the array angle  $\alpha$  is determined by choosing row-to-row offset ( $\delta$ ) and pitch ( $\lambda$ ) of the post array (defined in Fig. 1(b)) such that  $\tan(\alpha) = \delta/\lambda$ . For the examples given in Fig. 1 the array has an angle  $\alpha = 11.3^\circ$ , a post spacing  $G = 4 \mu\text{m}$ , post pitch  $\lambda = 11 \mu\text{m}$  and critical particle size of  $2.4 \mu\text{m}$ . Therefore,  $3.0 \mu\text{m}$  beads travel

along the array axis angle in the bumping mode and the  $0.5 \mu\text{m}$  beads travel along streamlines, as shown.

For the treatment aspect of the device to work properly, the lateral motion of the particle must outstrip the diffusion of the treatment chemical. As a bumping particle moves a distance  $L$  through the array, the particle should move a lateral distance,  $L\tan(\alpha) \sim \alpha L$ , that is greater than the characteristic length that any reagent species from the stream diffuses into the adjacent zone,  $\sqrt{Dt}$ . The time for this transport is  $t = L/V$  where  $V$  is the average fluid velocity. In analogy to the Peclet number  $Pe$  we define a dimensionless figure of merit  $M$  as the square of the ratio of these two lengths.

$$M \equiv \alpha^2 L^2 / (Dt) = \alpha^2 LV / D = \alpha^2 Pe$$

As a design criterion, this dimensionless number should be much greater than one. For the bead washing example given in Fig. 1(b), this parameter  $M$  is  $\sim 100$ . A more detailed analysis of particle washing to reduce contaminant concentrations to an acceptable level is given in the ESI.

## Conclusion

In summary, we have presented a versatile new tool for continuous-flow, on-chip biological processing. We can move particles across chemical streams having different reagent constituents, enabling sequential chemical operations to be performed on the particles. With this method we have demonstrated on-chip cell treatments such as labeling and washing, and bacterial chromosomal extraction. The washing capabilities of this method are particularly valuable because they allow many analytical or cell treatment procedures to be cascaded on a single chip while still effectively isolating their reagents from cross-contamination. We also identified critical parameters for successful device design. While we demonstrated biological processing in our device by directly manipulating cells on-chip, bead-based assays are also widely used in bio-analysis to extract, sort and identify analytes based on surface-specific interactions. This approach could also be used to efficiently direct functional beads through various reaction or sampling stages and washed for downstream analysis.

## Methods

### Microfluidic device fabrication and operation

The post arrays, inlet/outlet microchannels and reservoirs were fabricated in silicon wafers using standard microfabrication techniques. (PDMS replica molding of a silicon master can also be used.) Photomasks (Photosciences, Torrance, CA, USA) were designed using L-Edit (Tanner Research, Monrovia, CA, USA). Etching masks were formed on the silicon wafers using single-layer photolithography (Karl Suss, MA6) with AZ 5214 photoresist (AZ Electronic Materials, Branchburg, NJ, USA) and DI : MIF 312 (1 : 1) developer. Samples were deep etched using an STS ASE Multiplex tool (Newport, UK) for Deep Reactive Ion Etching (DRIE) with an optimized recipe that ensured vertical sidewalls and low sidewall scalloping (100 nm peak to peak) [ESI figure M1]. Scanning Electron Microscopy (LEO 1550 SEM) was used to characterize the etching recipes and measure array parameters such as post size, post-to-post

spacing and gaps. Through-wafer sandblasting was used to create inlet holes using 50  $\mu\text{m}$  diameter, aluminium oxide particles (PrepStart, Danville Engineering, San Ramon CA). Devices were sealed with a thin  $\sim 30\ \mu\text{m}$  layer of untreated PDMS film fixed to a glass coverslip backplane, allowing for repeated use of individual silicon devices. All devices were mounted in an acrylic jig connected to an external vacuum pump. Differential air pressure was used to control fluid flow through the chip. Pressure was varied in the range of 1–12 psi to achieve a wide range of flow speeds in the various devices from 50–500  $\mu\text{m s}^{-1}$ . Running buffer for fluorescent microspheres (Duke Scientific, Fremont, CA, USA) was filtered (Micropore), degassed, ultrapure DI water with 2 g  $\text{l}^{-1}$  pluronic F-108 (BASF, Florham Park, New Jersey, USA).

### Laser fluorescence microscopy

An inverted microscope (Nikon, TE2000) and a stereomicroscope (Nikon, SMZ) were used to image the motion of fluorescent particles and cells in the devices. High pressure mercury lamps and an argon-ion laser were used as excitation sources with matching fluorescence filter sets. For laser fluorescence, the source was multi-line (Spectra-Physics) with individual wavelength selection using an Acoustic-Optic Tunable Filter (AOTF-Neos Technologies, Melbourne, FL, USA). The laser spot was rapidly scanned with an x–y scanning mirror (Cambridge Technology, Lexington, MA, USA) to create a wide, uniform illuminated field. Filter sets (Chroma Technologies, Rockingham, VT, USA) were used for laser epifluorescent imaging of fluorescent beads and fluorescently labeled cells (488 nm, 568 nm excitation). Corresponding emission filters included green (525/50 nm, 605/50 nm, 565/50 nm and dual bandpass filter (525/568 nm). Images were recorded using a color Retiga 1300 CCD (QImaging, Surrey, BC, Canada) and a grayscale, IPentaMax ICCD (Princeton Instruments, Trenton, NJ) camera. Time exposures were acquired by both cameras as single images or sets of image files that were later compiled into video files. The color camera output was refreshed to the screen after each integration, allowing video to be recorded by an AVI real-time screen capture program (AVIscreenclassic, www.bobyte.com). The intensified CCD camera output was stacks of sequential integrated images. All image processing was done with ImageJ, NIH and included merging grayscale images into red and green channels for RGB output and stack processing including multiple frame sums or averaging.

### Preparation of blood cells

Venous, EDTA-anticoagulated blood (Oklahoma Blood Institute, Oklahoma City, OK, USA) was used as a source for platelets and lymphocyte white blood cells. The Ficoll-Paque (GE Healthcare) protocol was used to select lymphocytes and platelets from whole blood. Following the centrifuge step, the lymphocyte and platelet rich layer was pipetted out and resuspended in running buffer (AutoMACS, Miltenyi Biotech, Auburn, CA, USA), a phosphate buffer with 150 mM NaCl at pH 7.2 containing 0.09%  $\text{NaN}_3$ , 0.2% BSA. The solution was centrifuged to pellet the lymphocytes. The supernatant, containing platelets, was removed and used for on-chip platelet labeling. Suspended, unlabeled platelets (50  $\mu\text{L}$ ) were loaded into

the lower input reservoir. Platelets in the array tracked through a stream of phycoerythrin conjugated CD41 antibodies (PE-CD41, eBioscience, San Diego, CA, USA, diluted 1 : 1 with running buffer) loaded into the center channel inlet. Flowing dye and labeled platelets were visualized with a grayscale, intensified CCD camera using laser fluorescence microscopy at 488 nm with a 565/50 nm emission filter specific to the PE label. Following labeling, platelets were washed in a third stream of the original running buffer (AutoMACS).

### Preparation of bacteria cells

The protocol for preparing *E. coli* spheroplast bacteria for on-chip lysis was modified from ref. 18. First, a culture of GFP expressing *E. coli* (RP436) was grown overnight in 2 ml LB broth with 50  $\mu\text{g mL}^{-1}$  ampicillin. Then 400  $\mu\text{L}$  (OD usually between 1.0 and 1.5) of culture were pelleted and resuspended in 200  $\mu\text{L}$  Tris-buffered saline (0.05 M Tris, 0.138 M NaCl, 0.0027 M KCl, pH 8.0). SYTO 13 in DMSO (Invitrogen Corporation, Carlsbad, CA) was added to a final concentration of 0.5–1.0 mM to label the bacterial chromosome. The solution was then mixed gently by pipetting, and incubated for 20 min at room temperature. Labeled cells were then pelleted and resuspended in 200  $\mu\text{L}$  0.05 M Tris, 0.138 M NaCl, 0.0027 M KCl, and 0.5 or 1.125 M sucrose, pH 8.0. 1.0  $\mu\text{L}$  of 0.2 M EDTA and 5.0  $\mu\text{L}$  10 mg  $\text{mL}^{-1}$  lysozyme were added to digest the cell wall. After mixing by pipetting, the solution was incubated for 20 min at 37° C. This yields final buffer concentrations of: 0.05 M Tris, 0.138 M NaCl, 0.0027 M KCl, 1.125 M sucrose, 1 mM EDTA, 250  $\mu\text{g mL}^{-1}$  lysozyme. The microfluidic system was preloaded with this as running buffer. Spheroplasted *E. coli* cells were loaded into the lower inlet at low concentration. The detergent, SDS, was added to the upper reservoir to a final concentration of 8% by mass. The GFP and SYTO 13 dye were imaged simultaneously by epifluorescence with 488 nm argon-ion laser excitation at 525/50 emission filter. For the control experiment [ESI video M4†] showing cell lysis without the labeled chromosome GFP rich buffer was also loaded into a center input channel to trace the flow and to delineate the running buffer from cell lysing solution.

### Acknowledgements

We thank Cherry Ting for helpful discussions and preliminary experiments. This work was supported by the AFOSR, NIH (HG01506), NSF Nanobiology Technology Center (BSCECS9876771). It was also performed in part at the Cornell Nano-Scale Science and Technology Facility (CNF) which is supported by the National Science Foundation under Grant ECS-9731293, its users, Cornell University and Industrial Affiliates.

### Notes and references

- 1 L. R. Huang, E. C. Cox, R. H. Austin and J. C. Sturm, *Science*, 2004, **304**, 987–990.
- 2 B. H. Weigl and P. Yager, *Science*, 1999, **283**, 346–347.
- 3 J. B. Knight, A. Vishwanath, J. P. Brody and R. H. Austin, *Phys. Rev. Lett.*, 1998, **80**, 3863–3866.
- 4 P. J. A. Kenis, R. F. Ismagilov and G. M. Whitesides, *Science*, 1999, **285**, 83–85.

- 
- 5 T. M. Squires and S. R. Quake, *Rev. Mod. Phys.*, 2005, **77**, 977–1026.
  - 6 J. O. Tegenfeldt, *et al.*, *Anal. Bioanal. Chem.*, 2004, **378**, 1678–1692.
  - 7 P. Yager *et al.*, *Nature*, 2006, **442**, 412–418.
  - 8 J. Piper *et al.*, *Nat. Neurosci.*, 2007, **13**, 1259–1263.
  - 9 A. D. Stroock, *et al.*, *Science*, 2002, **295**, 647–651.
  - 10 H. Song, J. D. Tice and R. F. Ismagilov, *Angew. Chem.*, 2003, **42**, 767–772.
  - 11 D. Therriault, S. R. White and J. A. Lewis, *Nat. Mater.*, 2003, **2**, 265–271.
  - 12 J. Atencia and D. J. Beebe, *Nature*, 2005, **437**, 648–655.
  - 13 P. C. H. Li and D. J. Harrison, *Anal. Chem.*, 1997, **69**, 1564–1568.
  - 14 A. Y. Fu, H. P. Chou, C. Spence, F. H. Arnold and S. R. Quake, *Anal. Chem.*, 2002, **74**, 2451–2457.
  - 15 S. Takayama, *et al.*, *Chem. Biol.*, 2003, **10**, 123–130.
  - 16 J. Enger, *et al.*, *Lab Chip*, 2004, **4**, 196–200.
  - 17 D. Magde, E. L. Elson and W. Webb, *Biopolymers*, 1974, **13**, 29–61.
  - 18 C. Prinz, J. O. Tegenfeldt, R. H. Austin, E. C. Cox and J. C. Sturm, *Lab Chip*, 2002, **2**, 207–212.
  - 19 D. C. Birdsell and E. H. Cota-Robles, *J. Bacteriol.*, 1967, 427–437.
  - 20 D. W. Inglis, J. A. Davis, R. H. Austin and J. C. Sturm, *Lab Chip*, 2006, **6**, 655–658.
  - 21 J. A. Davis, *et al.*, *Proc. Natl. Acad. Sci. U. S. A.*, 2006, **103**, 14779–14784.
  - 22 K. J. Morton, J. C. Sturm, R. H. Austin and S. Y. Chou, *Proceedings of  $\mu$ TAS Conference*, 2006, vol. 1, pp. 1814–1817.